

# The safety band of Antarctic ice shelves

Johannes Jakob Fürst<sup>1,2\*</sup>, Gaël Durand<sup>1,2</sup>, Fabien Gillet-Chaulet<sup>1,2</sup>, Laure Tavard<sup>1,2</sup>, Melanie Rankl<sup>3</sup>, Matthias Braun<sup>3</sup> and Olivier Gagliardini<sup>1,2,4</sup>

**The floating ice shelves along the seaboard of the Antarctic ice sheet restrain the outflow of upstream grounded ice<sup>1,2</sup>. Removal of these ice shelves, as shown by past ice-shelf recession and break-up, accelerates the outflow<sup>3,4</sup>, which adds to sea-level rise. A key question in predicting future outflow is to quantify the extent of calving that might precondition other dynamic consequences and lead to loss of ice-shelf restraint. Here we delineate frontal areas that we label as 'passive shelf ice' and that can be removed without major dynamic implications, with contrasting results across the continent. The ice shelves in the Amundsen and Bellingshausen seas have limited or almost no 'passive' portion, which implies that further retreat of current ice-shelf fronts will yield important dynamic consequences. This region is particularly vulnerable as ice shelves have been thinning at high rates for two decades<sup>5</sup> and as upstream grounded ice rests on a backward sloping bed, a precondition to marine ice-sheet instability<sup>6,7</sup>. In contrast to these ice shelves, Larsen C Ice Shelf, in the Weddell Sea, exhibits a large 'passive' frontal area, suggesting that the imminent calving of a vast tabular iceberg<sup>8</sup> will be unlikely to instantly produce much dynamic change.**

The future fate of the Antarctic ice sheet under a warming climate is dynamically tied to geometric changes of the floating ice shelves. The reason is that ice shelves transmit buttressing to upstream regions<sup>1,2</sup>. Sources for buttressing are shearing at lateral confinements and positions where the ice shelf locally runs aground, such as at ice rises and ice rumples. As Antarctic ice shelves are known to be thinning<sup>9</sup> at increasing rates<sup>5</sup>, their buttressing potential is expected to reduce. Under continuous atmospheric warming over the Antarctic Peninsula<sup>10</sup>, vast ice-shelf areas have already been lost. Before break-up, ice shelves accommodated a certain gradual recession of the ice front<sup>11–14</sup>. During this recession, a transition of the calving front was observed from being convex to becoming concave, reaching either further or less out into the ocean between any anchor points. After break-up, the extant glacier fronts were no longer buttressed and tributary glaciers accelerated<sup>15,16</sup> with, in places, an eightfold velocity increase<sup>3</sup>. This had direct consequences for ice flowing over the boundary between grounded and floating ice—that is, the ice discharge over the grounding line. More than one decade after the major break-up events on the Antarctic Peninsula, glaciers still adjust to these past perturbations<sup>4</sup>.

To this day, it remains largely unquantified which parts of the floating area are more or less important for the overall dynamic state of an ice shelf. For this purpose, we quantify the buttressing effect and delineate the ice-shelf area which has little or no dynamical influence. This area is referred to as passive shelf ice (PSI). Our quantification of buttressing relies on the stress regime within the ice<sup>17</sup>, which is inferred from a state-of-the-art data assimilation

into an ice-flow model<sup>18–20</sup> (Supplementary Section 1). From the stress field, buttressing is calculated as a normal force exerted by the ice shelf on upstream ice in a given horizontal direction<sup>17</sup> (Supplementary Section 2.1). This force is compared to the vertically integrated hydrostatic pressure, a normal force, that the ocean water would exert if the ice shelf was removed up to this position. The ratio of these two forces determines the buttressing potential of the ice shelf. If both are equal, shelf ice is unbuttressed, as it neither provides nor transmits any extra restraint other than the ocean pressure. The required direction choice is made so that buttressing becomes maximal (Fig. 1). The reason for this choice is that low values in maximum buttressing point out regions that are not well buttressed in any direction and it is there that we suspect to encounter PSI. As we consider ice flow to be vertically homogeneous<sup>21</sup>, maximum buttressing is attained in the direction aligned with the second principal stress. On account of this direction choice, the 'compressive arch' criterion<sup>22</sup> might seem similar. Yet this arch is inferred from strain rates and it was introduced as an ice-shelf stability criterion. Here, the stability issue is not addressed and the buttressing primarily serves to identify PSI. Larsen C Ice Shelf shows a typical pattern of maximum buttressing, spanning the full range from being highly buttressed to unbuttressed (Fig. 2). Values generally decrease towards the ice front unless other geometric confinements are encountered, such as Bawden and Gipses ice rises. Near these two ice rises, buttressing is elevated as ice locally runs aground. Isolated patches of low buttressing are found at the lee side of promontories or where ice flow leaves a zone of lateral confinement.

From maximum buttressing, we infer a PSI-threshold that will serve to delineate the PSI area. For this, we performed generic calving experiments, along isolines in maximum buttressing, and looked at the instantaneous velocity response of individual ice-shelf regions (Supplementary Section 2.2). As long as there is no speed-up, we consider the removed ice as dynamically passive. When the flux over the ice front shows a step increase under successive calving, the PSI-threshold is passed. In this way, the delineation of PSI area is a diagnostic exclusively based on and representative of the present-day geometry and the present-day dynamic state of the ice shelves. As ice-shelf geometries evolve, their buttressing potential will alter in the long run. However, thinning within the PSI area is found to leave the upstream buttressing regime and with it the delineation of PSI area unaffected. For Larsen C, the PSI-threshold lies at 0.3, implying that 10.3% (or ~6,000 km<sup>2</sup>) of the total area contains PSI. Once calving exceeds the PSI area, the ice shelf accelerates, but this does not necessarily imply an instant increase in tributary-glacier discharge. Such an increase is confirmed when 55% (or ~30,000 km<sup>2</sup>) of the ice-shelf area is lost. A propagating rift on Larsen C overcame a stabilizing zone of soft ice in 2014, which gave

<sup>1</sup>CNRS, Laboratoire de Glaciologie et Géophysique de l'Environnement (LGGE), UMR 5183, Grenoble, France. <sup>2</sup>Université Grenoble Alpes, LGGE, UMR 5183, Grenoble, France. <sup>3</sup>Institute of Geography, University of Erlangen-Nuremberg, Erlangen, Germany. <sup>4</sup>Institut Universitaire de France, Paris, France. \*e-mail: johannes.fuerst@lgge.obs-ujf-grenoble.fr; johannes.fuerst@fau.de

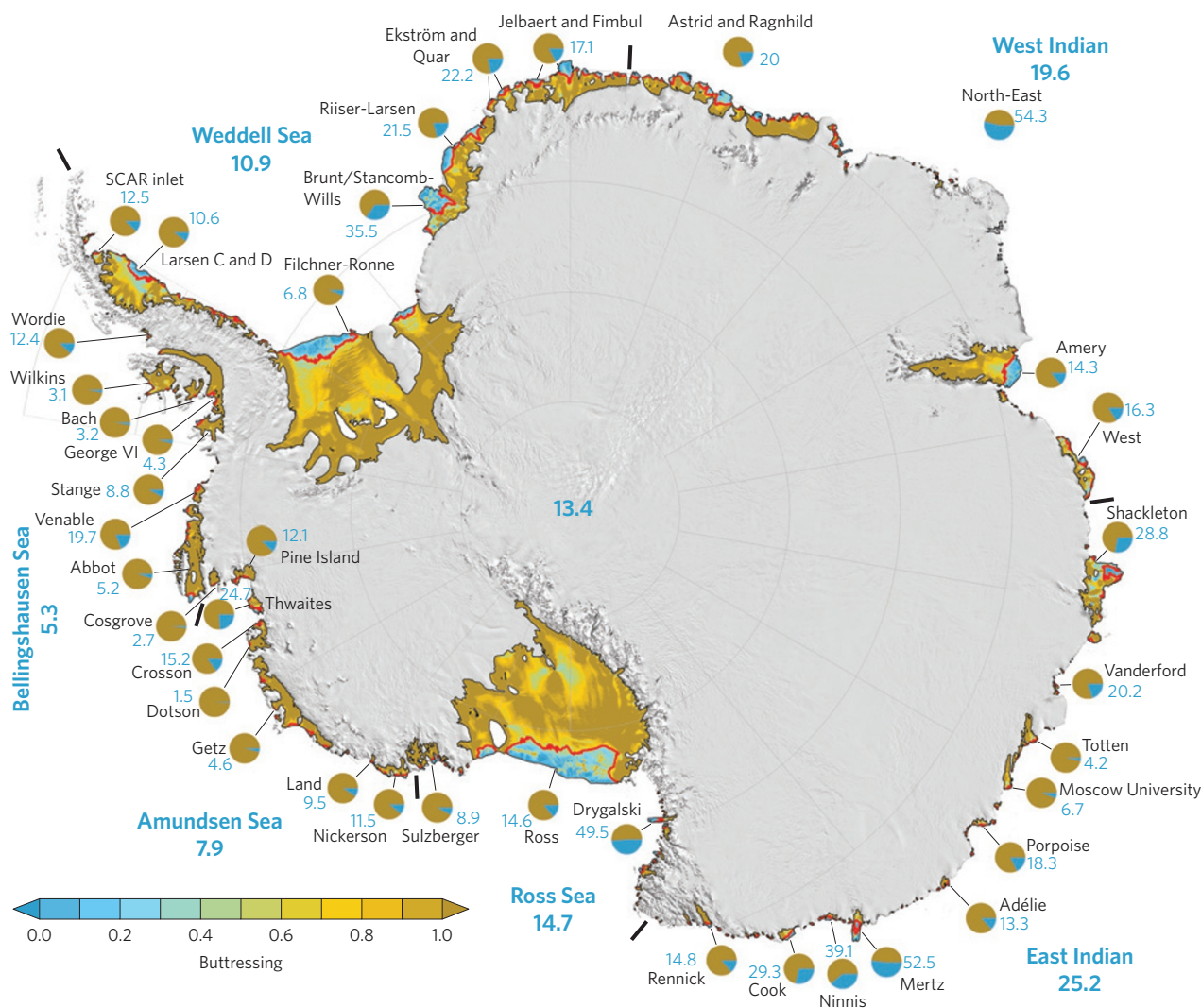


**Figure 1 | Maximum buttressing of Antarctic ice shelves.** The field serves to infer the extent of the PSI area (red contours). For the labelled ice-shelf regions, we computed PSI-area percentages (pie charts and blue numbers). Regional percentage values (bold blue numbers) are given for six sectors (separated by black bars) and for the whole of Antarctica. Maximum buttressing is less informative further upstream, where values exceed 1. There, spatial differences, in how much grounded ice outflow is restrained, are deducible from buttressing quantified in flow direction (Supplementary Section 2.1). Red contours are smoothed (4-km moving average). Black contours delineate floating areas. Background map data from ref. 31; 2008–2009 MODIS Mosaic.

rise to concerns on the dynamic integrity of the ice shelf<sup>8</sup>. If further propagation of the ice rift triggered a calving event, it will mostly remove passive shelf ice. From the buttressing regime, we anticipate no significant ice-shelf speed-up, let alone an abrupt increase in ice discharge. However, the ice front will take on a concave shape, a state that all former northern parts of Larsen Ice Shelf adopted before their respective break-up<sup>11–14</sup>. Even if Larsen C detached from Bawden Ice Rise, an instant ice discharge increase is not confirmed, although a large portion of the ice shelf accelerates (Supplementary Section 3.1).

A first proof of principle in the observational record comes from Mertz Glacier. In 2010, more than half of its floating ice tongue (~55%) calved off as a vast tabular iceberg without causing a significant acceleration of the extant glacier trunk<sup>23</sup>. Our buttressing analysis provides an explanation, as the lost portion primarily contained PSI, which constituted 52.5% of the glacier tongue before calving (Fig. 1). A second indication for the applicability of the PSI concept is provided by the major calving event in 2008 on Wilkins Ice Shelf<sup>24</sup> that partially removed a buttressed ice bridge. Before calving, ~3% of the area contained PSI. Calving cut into highly buttressed ice and should have caused an acceleration.

Satellite observations confirm that the ice-shelf front sped up, but the acceleration did not extend far beyond prominent ice rises (Supplementary Section 3.2).

For the whole of Antarctica, we find a 13.4% PSI-area fraction (Fig. 1), which we consider a safety band under future ice-front retreat. The fraction of the PSI area also gives an indication of the ice-front shape. On the one hand, five out of the seven ice shelves with a PSI-area fraction below 5% have concave or rather straight ice fronts. On the other hand, well-expressed convex ice fronts prevail for PSI-area fractions exceeding ~10%. Outstanding in terms of a large relative PSI-area extent are the ice tongues of Mertz and Drygalski glaciers, with 52.5% and 49.5%, respectively. These ice tongues are largely unconfined outside the narrow glacier embayment and kept in place by prolific inflow from upstream. Apart from such unconstrained ice tongues, ice shelves can also show a relatively large PSI area. Prominent examples are Brunt/Stancomb-Wills and Shackleton ice shelves, with 35.5 and 28.8% of their respective total areas being removable without major consequences for the upstream ice flow. The smallest PSI-area fractions are found for Cosgrove (2.7%) and Dotson (1.5%) ice shelves, both located in the Amundsen Sea sector.



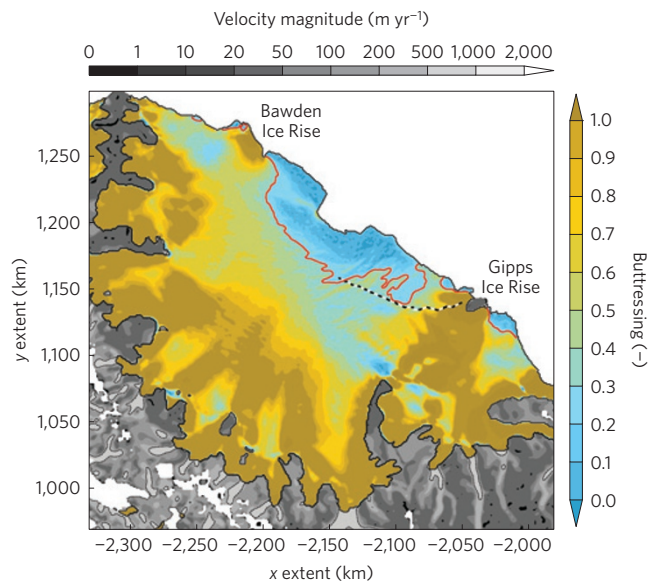


**Figure 2 | Maximum buttressing on Larsen C Ice Shelf.** Low values are found in areas that are generally not well buttressed, and this is where we suspect PSI would be found. For Larsen C, the 0.3 isoline in maximum buttressing is found to delineate the PSI area (red contours). The calving event that is presumably triggered by a rift that continuously opened and propagated in 2014 (ref. 8; black-white dashed line), will mostly remove PSI. Grey shading gives observed surface-velocity magnitudes for grounded ice, with the 100-m yr<sup>-1</sup> isoline being highlighted (black dashed lines). Red contours are smoothed as in Fig. 1.

On a regional level, there are clear differences in terms of the PSI extent. Ice shelves in the Indian Ocean sector (Fig. 1) show on average a ~20% PSI-area fraction. Along the coast of Queen Maud Land, ice shelves also exhibit this 20% PSI-area fraction, yet their values are very homogeneous. There, this 'healthy' PSI portion coincides with conspicuously low subsurface melt rates, well below 1 m yr<sup>-1</sup> for individual ice shelves<sup>25,26</sup>. Conversely, we find substantial melt rates in the Amundsen and Bellingshausen sea sectors, where regional PSI-area fractions are 7 and 5%, respectively, both well below the Antarctic average. Although this might suggest a link between melt rates and PSI-area fraction, the relation breaks down for other regions, and certainly for individual ice shelves. Considering uncertainties on parameters and observations, a sensitivity analysis (Supplementary Section 2.3) indicates that the inferred regional differences are very robust.

Ice shelves with little PSI demand detailed monitoring of thickness changes and fracture formation, as further calving is likely to cut into the dynamically relevant areas. These susceptible ice shelves are primarily found in the Amundsen and Bellingshausen sea sectors, where we identify not only six out of the seven ice shelves with a PSI-area fraction smaller than 5%, but also the four smallest PSI-area fractions (Fig. 1). Any further recession of ice fronts there is likely to entail a non-negligible acceleration of the floating parts. In this regard, it is alarming that ice shelves in the Amundsen and Bellingshausen seas not only experienced the highest rates of subsurface melting<sup>25–27</sup>, but also that thinning accelerated during the past two decades<sup>5</sup>. Thinning was most pronounced for Dotson, Crosson, Thwaites, Pine Island and Venable, where ice-shelf-wide loss rates exceed 2 m yr<sup>-1</sup> (ref. 5). For the ice shelf of Pine Island Glacier, calving beyond the PSI area is found to have an immediate effect on the ice discharge (Supplementary Table 1). Increased ice discharge will probably drive the grounding line inland. Further concerns are raised by the fact that outlet glaciers in the Amundsen Sea Embayment primarily rest on retrograde bed slopes,

a geometric prerequisite for the marine ice-sheet instability<sup>6,7</sup>. This dynamic instability implies a self-sustained grounding-line retreat and outflow acceleration.

From our buttressing analysis, we identified PSI in 13.4% of the floating areas around the whole of Antarctica (Fig. 1). The inferred buttressing regime is an inherent property of the viscous ice-shelf flow and exclusively based on the present dynamic and geometric state. Free of information and assumptions on the mechanisms that drive ice-shelf weakening and retreat, buttressing can serve to impartially assess dynamic implications in response not only to frontal calving but also to more gradual perturbations from surface and subsurface melting<sup>25–28</sup>. In the PSI area, our analysis suggests no important dynamic consequences from such gradual ice loss. Outside the PSI area, melting will affect the buttressing potential. Consequences for upstream tributary glaciers are then best estimated from buttressing in flow direction (Supplementary Section 2.1). As long as ice shelves do not unground from a contact with the seabed, ice flow is expected to adjust gradually in accordance with the melting signal. Furthermore, it is known that melting occurs along the grounding line deep in the sub-ice-shelf cavity<sup>27</sup>. If subsurface melting there is not in balance with ice flow, as for instance in the Amundsen Sea Embayment, or if melting there intensifies in the future as a response to changing ocean currents under climatic warming<sup>29</sup>, buttressing will be considerably reduced where it matters most for ice dynamics<sup>30</sup>. Analysing the buttressing of entire ice shelves can then serve to pin down regions where dynamic consequences from melting may primarily manifest.

**Data availability.** Buttressing fields and other variables derived from the underlying data assimilation are stored at the National Snow and Ice Data Center (NSIDC). The dataset is entitled 'SUMER Antarctic ice-shelf buttressing' (<http://dx.doi.org/10.5067/FWHORAYVZCE7>).

Received 2 August 2015; accepted 4 December 2015;  
published online 8 February 2016

## References

- Dupont, T. K. & Alley, R. B. Assessment of the importance of ice-shelf buttressing to ice-sheet flow. *Geophys. Res. Lett.* **32**, L04503 (2005).
- Gagliardini, O., Durand, G., Zwinger, T., Hindmarsh, R. C. A. & Le Meur, E. Coupling of ice-shelf melting and buttressing is a key process in ice-sheet dynamics. *Geophys. Res. Lett.* **37**, L14501 (2010).
- Rignot, E. *et al.* Accelerated ice discharge from the Antarctic Peninsula following the collapse of Larsen B Ice Shelf. *Geophys. Res. Lett.* **31**, L18401 (2004).
- Berthier, E., Scambos, T. A. & Shuman, C. A. Mass loss of Larsen B tributary glaciers (Antarctic Peninsula) unabated since 2002. *Geophys. Res. Lett.* **39**, L13501 (2012).
- Paolo, F. S., Fricker, H. A. & Padman, L. Volume loss from Antarctic ice shelves is accelerating. *Science* **348**, 327–331 (2015).
- Weertman, J. Stability of the junction of an ice sheet and an ice shelf. *J. Glaciol.* **13**, 3–11 (1974).
- Schoof, C. Ice sheet grounding line dynamics: steady states, stability, and hysteresis. *J. Geophys. Res.* **112**, F03S28 (2007).
- Jansen, D. *et al.* Brief communication: newly developing rift in Larsen C Ice Shelf presents significant risk to stability. *Cryosphere* **9**, 1223–1227 (2015).
- Pritchard, H. D. *et al.* Antarctic ice-sheet loss driven by basal melting of ice shelves. *Nature* **484**, 502–505 (2012).
- O'Donnell, R., Lewis, N., McIntyre, S. & Condon, J. Improved methods for PCA-based reconstructions: case study using the Steig *et al.* (2009) Antarctic temperature reconstruction. *J. Clim.* **24**, 2099–2115 (2011).
- Skvarca, P. Changes and surface features of the Larsen Ice Shelf, Antarctica, derived from Landsat and Kosmos mosaics. *Ann. Glaciol.* **20**, 6–12 (1994).
- Rott, H., Skvarca, P. & Nagler, T. Rapid collapse of northern Larsen Ice Shelf, Antarctica. *Science* **271**, 788–792 (1996).
- Vaughan, D. G. & Doake, C. S. M. Recent atmospheric warming and retreat of ice shelves on the Antarctic Peninsula. *Nature* **379**, 328–331 (1996).
- Scambos, T. A., Hulbe, C. A. & Fahnestock, M. *Antarctic Peninsula Climate Variability: Historical and Paleoenvironmental Perspectives* (American Geophysical Union, 2013).

15. De Angelis, H. & Skvarca, P. Glacier surge after ice shelf collapse. *Science* **299**, 1560–1562 (2003).
16. Seehaus, T., Marinsek, S., Helm, V., Skvarca, P. & Braun, M. Changes in ice dynamics, elevation and mass discharge of Dinsmoor–Bombardier–Edgeworth glacier system, Antarctic Peninsula. *Earth Planet. Sci. Lett.* **427**, 125–135 (2015).
17. Gudmundsson, G. H. Ice-shelf buttressing and the stability of marine ice sheets. *Cryosphere* **7**, 647–655 (2013).
18. Morlighem, M. *et al.* Spatial patterns of basal drag inferred using control methods from a full-Stokes and simpler models for Pine Island Glacier, West Antarctica. *Geophys. Res. Lett.* **37**, L14502 (2010).
19. Gillet-Chaulet, F. *et al.* Greenland ice sheet contribution to sea-level rise from a new-generation ice-sheet model. *Cryosphere* **6**, 1561–1576 (2012).
20. Fürst, J. J. *et al.* Assimilation of Antarctic velocity observations provides evidence for uncharted pinning points. *Cryosphere* **9**, 1427–1443 (2015).
21. Morland, L. W. *Dynamics of the West Antarctic Ice Sheet* (Kluwer Acad., 1986).
22. Doake, C. S. M., Corr, H. F. J., Rott, H., Skvarca, P. & Young, N. W. Breakup and conditions for stability of the northern Larsen Ice Shelf, Antarctica. *Nature* **391**, 778–780 (1998).
23. Massom, R. A. *et al.* External influences on the Mertz Glacier Tongue (East Antarctica) in the decade leading up to its calving in 2010. *J. Geophys. Res.* **120**, 490–506 (2015).
24. Braun, M., Humbert, A. & Moll, A. Changes of Wilkins Ice Shelf over the past 15 years and inferences on its stability. *Cryosphere* **3**, 41–56 (2009).
25. Depoorter, M. A. *et al.* Calving fluxes and basal melt rates of Antarctic ice shelves. *Nature* **502**, 89–92 (2013).
26. Rignot, E., Jacobs, S., Mouginot, J. & Scheuchl, B. Ice-shelf melting around Antarctica. *Science* **341**, 266–270 (2013).
27. Dutrieux, P. *et al.* Pine Island Glacier ice shelf melt distributed at kilometre scales. *Cryosphere* **7**, 1543–1555 (2013).
28. Kuipers Munneke, P., Lightenberg, S. R. M., van den Broeke, M. R. & Vaughan, D. G. Firn air depletion as a precursor of Antarctic ice-shelf collapse. *J. Glaciol.* **60**, 205–214 (2014).
29. Hellmer, H. H., Kauker, F., Timmermann, R., Determann, J. & Rae, J. Twenty-first-century warming of a large Antarctic ice-shelf cavity by a redirected coastal current. *Nature* **485**, 225–228 (2012).
30. Bindschadler, R. Climate change—hitting the ice sheets where it hurts. *Science* **311**, 1720–1721 (2006).
31. Scambos, T., Haran, T., Fahnestock, M., Painter, T. & Bohlander, J. MODIS-based mosaic of Antarctica (MOA) data sets: continent-wide surface morphology and snow grain size. *Remote Sens. Environ.* **111**, 242–257 (2007).

## Acknowledgements

This study received primary funding from the French National Research Agency (ANR) under the SUMER (Blanc SIMI 6) 2012 project referenced as ANR-12-BS06-0018. Results presented in this publication are based on numerical simulations conducted either at CIMENT (Calcul Intensif Modélisation Expérimentation Numérique et Technologique), the high-performance computing centre of the Grenoble University, which is supported on local, county and regional levels via the CIRA project (Calcul intensif en Rhône Alpes), or at the CINES (Centre Informatique National de l'Enseignement Supérieur) computing centre under allocation 2015-016066 from GENCI (Grand Equipement National de Calcul Intensif). Results presented here also received support and benefited from the Elmer/Ice development team at the CSC-IT Center for Science Ltd (Finland). The velocity analysis on Wilkins was funded by the German Research Foundation (DFG) within the priority programme 1158 Antarctic Research under contract number BR2105/8-1 and as co-funded action to the HGF Alliance Remote Sensing and Earth System Dynamics. During the revision phase of the manuscript, the first author received funding from the DFG-project FU1032/1-1.

## Author contributions

G.D. initiated the quantification of ice-shelf buttressing and J.J.F. elaborated on it with a focus on identifying passive shelf ice. J.J.F. led the writing of the manuscript, in which he received support from all authors. The data assimilation was realized by J.J.F. and the Antarctic-wide calving experiments were designed and conducted by J.J.F. The research was directed in constant discussion with G.D., F.G.-C. and O.G. Software maintenance and technical support from L.T. was essential to render the conducted experiments possible. Velocities of Wilkins Ice Shelf were inferred and provided by M.R. and M.B.

## Additional information

Supplementary information is available in the [online version of the paper](#). Reprints and permissions information is available online at [www.nature.com/reprints](http://www.nature.com/reprints). Correspondence and requests for materials should be addressed to J.J.F.

## Competing financial interests

The authors declare no competing financial interests.